# CMS ECAL Calibration Strategy

Georgios Daskalakis

*Imperial College, London, UK*

**Abstract.** The CMS Electromagnetic crystal Calorimeter (ECAL) must be precisely calibrated if its full potential performance is to be realized. Inter-calibration from laboratory measurements and cosmic ray muons will be available for all crystals and has been demonstrated to give good pre-calibration values at the start-up; some crystals will be also inter-calibrated using an electron beam. *In-situ* calibration with physics events will be the main tool to reduce the constant term of the energy resolution to the design goal of 0.5%. In the following the calibration strategy will be described in detail.

**Keywords:** CMS, ECAL, calibration, calorimeter, crystals, in-situ, electrons, lead tungstent
**PACS:** 06.20.Fn, 07.20.Fw

## The ECAL Detector

The ECAL [1] is made out of 75848 lead tungstate ($PbWO_4$) crystals (Fig. 1a). They are arranged into a Barrel (61200 crystals), covering the central rapidity region ($|\eta| < 1.5$) and two Endcaps (7324 crystals each) which extend the coverage (up to $|\eta| < 3.0$). Due to the high density (8.28 g/cm$^3$) and the small radiation length ($X_0 = 0.89$ cm) of $PbWO_4$, the calorimeter is very compact and can be placed inside the magnetic coil [2] needed for precise momentum measurements with the Tracker [3] and the Muon [4] systems. The small value of the Molière radius (2.2 cm) matches well the very fine granularity needed by the high particle density of the events at LHC. Crystals are organized in a quasi-projective geometry [1], which improves the hermeticity of the detector.

The electrons lose energy via bremsstrahlung in the Tracker material (Fig. 1b) while the photons are converted into electron pairs. In addition, the strong magnetic field bends the electrons causing the radiated energy to spread in $\varphi$. Both effects impact electron/photon energy resolution making the *in-situ* calibration of ECAL a challenge. Special reconstruction algorithms [5] have been developed to recover the radiated energy from electrons and to reconstruct the converted photons.

## ECAL Calibration

The physics reach of the ECAL, in particular the discovery potential for a low mass Standard Model Higgs boson in the two photon decay channel [6], depends on its excellent energy resolution.

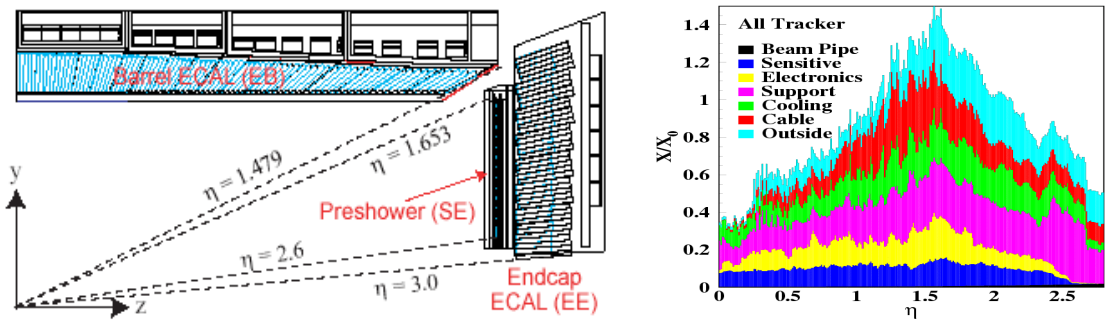


(a) (b)

**FIGURE 1.** (a) A slice through a quadrant of the CMS Electromagnetic Calorimeter (b) the Tracker material distribution in front of the ECAL.

The intrinsic ECAL energy resolution measured in Testbeam (by summing the deposited energy in a 3×3 array of crystals around the crystal in beam) is expressed by the following parameterization (E is in GeV):

$$\left(\frac{\sigma}{E}\right)^2 = \left(\frac{2.9\%}{\sqrt{E}}\right)^2 + \left(\frac{125(MeV)}{E}\right)^2 + (0.30\%)^2 \qquad (1)$$

which matches the design resolution for a perfectly calibrated detector. Mis-calibration will directly affect the constant term, degrading the overall ECAL performance.

The goal of the calibration strategy is to achieve the most accurate energy measurement for electron and photons. Schematically, the reconstructed energy can be decomposed into three factors [5]:

$$E_{e,\gamma} = G \times F \times \sum_{i}^{Cluster} c_i \times A_i \qquad (2)$$

where $G$ is a global absolute scale and $F$ accounts for energy losses due to bremsstrahlung and containment variations. The $c_i$ factors are the inter-calibration coefficients while the $A_i$ are the signal amplitudes, in ADC counts, which are summed over the clustered crystals. The main source of channel-to-channel response variation in the Barrel is the crystal-to-crystal variation of scintillation light yield which has an r.m.s. of ~15%. In the Endcaps, the crystal signal yield and the product of the gain, quantum efficiency and the photocathode area of the VPTs, have an r.m.s. variation of almost 25%.

The target inter-calibration precision can only be achieved using physics events. Over the period of time in which the physics events used to provide an inter-calibration are taken, the calorimeter response ideally should remain stable and constant to high precision. One source of significant variation is changes in crystal transparency caused by irradiation and subsequent annealing. The changes are tracked and corrected using a laser monitoring system [7]. In addition, the sensitivity of both crystal and photo-detector response to temperature fluctuations requires a precise control of the temperature stability. The water-cooling system guarantees a long-term temperature stability of the crystal volume and the APDs below the 0.1 $^{o}$C level [7], in order to be able to meet the target values for the energy resolution.

## Calibration Roadmap

There are two distinct periods during which calibration can be performed. The first period is before the installation of the detector. During that period ECAL crystals can be calibrated in Testbeam (around 10k crystals only, due to the restricted beam time), using light yield measurements in the laboratories that check the crystals quality and by using cosmic muons. When the detector will be fully operational, minimum bias events and/or Level-1 jet triggers could be used in order to achieve a fast crystal inter-calibration. Precise *in-situ* inter-calibration can be achieved with isolated electrons from sources like $W \rightarrow e\nu$ or $Z \rightarrow e^+e^-$ decays. The absolute calibration scale as well as other calibration tasks can be achieved by using the mass constraint for electrons from $Z \rightarrow e^+e^-$ decays. There is also the possibility to achieve a fast and accurate calibration using $\pi^0, \eta \rightarrow \gamma\gamma$ or $Z \rightarrow \mu\mu\gamma$ decays.

## Calibration in Testbeam

In the Testbeam, supermodules [1] are mounted on a rotating table that allows rotation in both the $\eta$ and $\varphi$ coordinates and are fully scanned with high-energy electron beams. The incident electron positions are measured with a set of hodoscopes. The response of a single crystal to electrons depends on the electron incident position. The dependence on the two lateral coordinates can be factorized and corrected. The inter-calibration coefficients $c_i$ for crystal $i$ are defined as the ratio of the mean value of the corrected response to a reference value.

The statistical uncertainty remains negligible (less than 0.1%) provided that at least 1000 events are taken per crystal. The inter-calibration precision, when these constants are used *in-situ*, is expected to be limited by variations occurring in the time between their determination in the Testbeam and their utilization in the installed detector.

## Calibration from Laboratory Measurements

The crystal calorimeter is being assembled in 2 regional centers: at CERN and at INFN-ENEA Casaccia near Rome. During the assembly phase, all the detector components are characterized and the data are saved in the construction database. From these data it is possible to estimate the inter-calibration coefficients $c_i$ of each channel $i$ as [7]:

$$\frac{1}{c_i} \sim LY \cdot \varepsilon_Q \cdot c_{ele} \cdot M,$$

where $LY$ is the Light Yield of the crystals, $M$ and $\varepsilon_Q$ are respectively the gain and quantum efficiency of the photo-detectors and $c_{ele}$ is the calibration of the electronics chain. The crystal $LY$ is measured in the laboratory with a photo-multiplier tube, exciting the crystal with a $^{60}Co$ source that emits photons with energy of 1.2 MeV. This gives an average $LY_{PMT}$ for the $PbWO_4$ crystals of 10 pe/MeV at 18 $^oC$. The

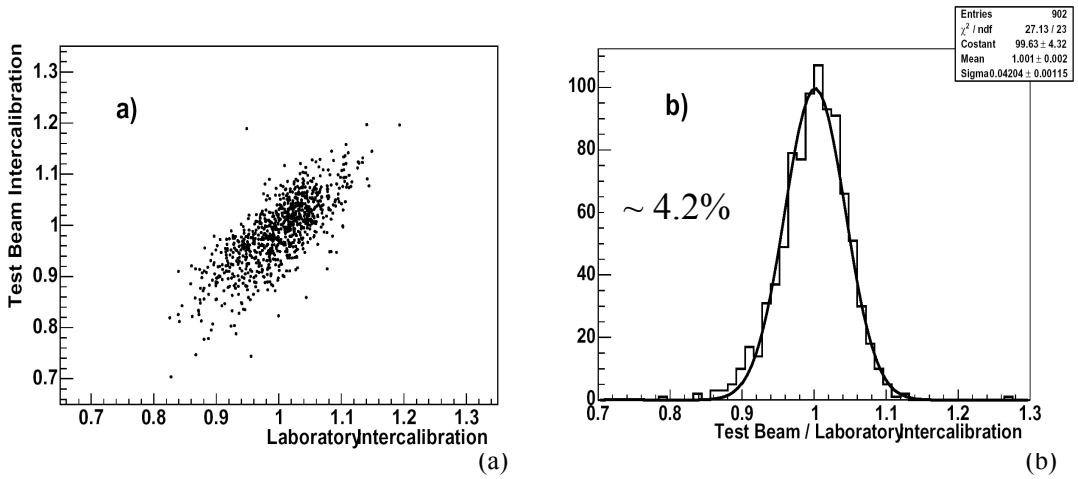


**FIGURE 2.** (a) Inter-calibration coefficients obtained in Testbeam versus those obtained from laboratory measurements (b) ratio between Testbeam and laboratory inter-calibration coefficients.

measurements span about 7 years of crystal production.

In order to establish the inter-calibration precision achieved with the laboratory measurements, the inter-calibration coefficients are compared with those from Testbeam measurements (Fig. 2a). As can be seen from their ratio (Fig. 2b) an inter-calibration precision of about 4.2% can be obtained from laboratory measurements.

## Calibration with Cosmic Ray Muons

Inter-calibration coefficients for Barrel crystals are also obtained using cosmic muons that are well aligned with the crystal axes [8]. For this measurement the APD gain is increased by a factor 4 with respect to the gain to be used during normal data taking by increasing the bias voltage. This improves the signal to noise ratio and allows the selection of muons passing through the full length of crystals by vetoing on signals in surrounding crystals. An overall precision of 3.0-3.5% should be achievable in one week of data taking. The statistical contribution to the overall uncertainty was estimated to be around 2%.

## Calibration with the φ – uniformity Method

The proposed technique makes use of the φ-uniformity of deposited energy to inter-calibrate crystals within rings at constant η. Due to the symmetry of the ECAL about η=0, crystals with same |η| are folded. In the Barrel, there are 85 pairs of rings with 360 crystals per ring. In the Endcaps, there are 39 pairs of rings and the number of crystals per ring varies with η.

Inter-calibration is performed by comparing the total energy deposited in each crystal with the mean of the distribution of total energies for all crystals in a ring. For the moment, two choices of event trigger have been investigated: random bunch crossings [9], and Level-1 jet triggers [10]. The inter-calibration precision for a

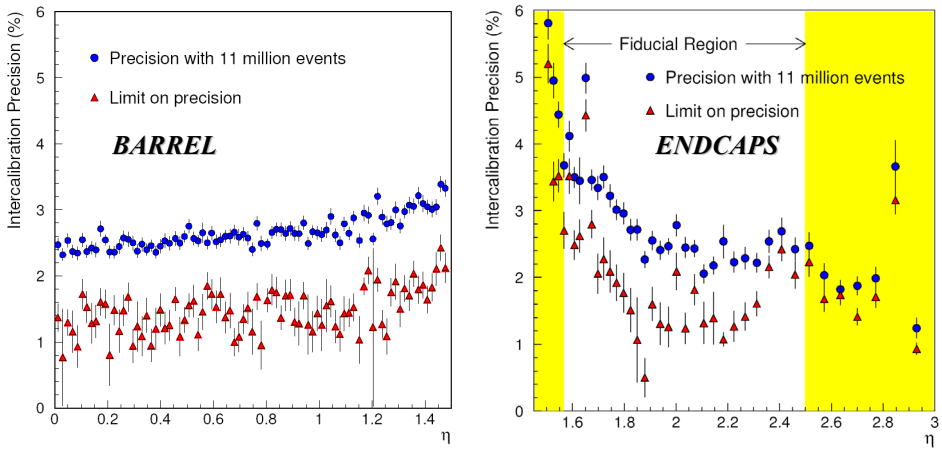


(a) (b)

**FIGURE 3.** Inter-calibration precision achieved with the φ-uniformity method (a) in the ECAL Barrel and (b) in the ECAL Endcaps, obtained with 11 millions Level-1 jet trigger simulated events (circles). The expected limit on the inter-calibration precision is also shown (triangles).

given $|\eta|$ is obtained from the Gaussian width of the distribution of $\Sigma E_T$ for the pair of rings of crystals at that value of $|\eta|$.

A limit on the precision arises due to non-uniformities in φ, primarily from the in-homogeneity of Tracker material, but also from geometrical asymmetries such as the varying off-pointing angle of Endcap crystals, and the boundaries between Barrel supermodules.

Results based on a Level-1 jet-triggers simulated sample are shown in Fig. 3a for the Barrel and in Fig. 3b for the Endcaps. It can be seen that without using any knowledge about the material distribution in the Tracker, the limit on the precision is close to 1.5% throughout the Barrel and between 3.0% and 1.0% for the fiducial region of the Endcaps. It is expected that the limit on the precision will be closely approached with a few tens of millions of events. This is equivalent to about 10 hours of data taking, under the assumption that 1 kHz of Level-1 bandwidth is allocated to single jet triggers, and that the calibration software has access to this rate, either running on the Filter Farm, or more probably, running offline on a highly compacted data stream (a few tens of channels stored per event).

## Calibration with $Z \rightarrow e^+e^-$

The Z mass constraint in $Z \rightarrow e^+e^-$ decays is a powerful tool for calibration. A number of different uses are envisaged, from tuning the corrections of the electron reconstruction algorithms as shown in [11], to the inter-calibration of regions of the ECAL, for example as a complement to the φ-uniformity method at the start-up.

For a preliminary estimate of the inter-calibration factors between rings, electrons that radiated little were chosen since their reconstructed energy shows the least dependence on the Tracker material, and hence η. The method has been tested taking the calorimeter regions as rings of crystals (at fixed η) in the ECAL Barrel. The results obtained when starting from a 5% mis-calibration between rings and a 2% mis-

calibration between crystals within a ring, using events corresponding to an integrated luminosity of 2.0 $fb^{-1}$, corresponds to 0.6% ring inter-calibration precision.

## Calibration with Isolated Electrons

Once the Tracker is fully operational and well aligned, inter-calibration of crystals can be performed using the momentum measurement of isolated electrons [12]. The main difficulty in using electrons for inter-calibration is that electrons radiate in the Tracker material in front of the ECAL, and both the energy and the momentum measurement (P) are affected. Moreover the average amount of bremsstrahlung varies with Tracker material thickness. The ECAL energy will be measured by summing the energy deposited in the 5×5 array of crystals (S25) around the crystal with the maximum signal. The energy in the 5×5 array does not require the complexity of a single crystal containment correction and helps in cleanly separate the inter-calibration from the corrections required by the super-clustering algorithms. In the Endcap, the energy measured in the Preshower and associated with the electron cluster is added to the energy summed in the crystals.

In order to extract the inter-calibration constants the individual crystal contributions must be unfolded, while minimizing the difference between the energy and momentum measurements. Two algorithms to achieve this minimization have been tested: an iterative technique that was used for the *in-situ* calibration of the BGO crystals in the L3/LEP experiment and a matrix inversion algorithm. The results, both in terms of precision and in terms of speed of algorithm, are similar, and show no dependence on the technique used. The event selection was based on variables that are sensitive to the amount of bremsstrahlung emission, chosen to select events with little bremsstrahlung.

Due to the variation of the average value of S25/P with pseudorapidity, caused by the variation of the amount of material in front of the ECAL, the calibration task will be divided into two steps. In the first step crystals in small regions in $\eta$, over which the average value of the S25/P is rather constant, will be inter-calibrated. In the second step the small regions will be inter-calibrated with each other.

The calibration precision versus $\eta$ achievable for a fixed integrated luminosity follows the Tracker material budget distribution (Fig. 4a). The simulated data used to obtain these results correspond to about 5(7) $fb^{-1}$ in the Barrel(Endcaps). This estimation uses the PYTHIA cross section for the W-production with no k-factor. The calibration precision was also extensively studied in different $\varphi$-regions keeping the same $\eta$ interval. There is no evidence of any $\varphi$-dependence.

The calibration precision achievable is strongly dependent on the number of electrons collected per crystal (HLT output). In Fig. 4b the inter-calibration precision versus the number of electrons per crystal is shown for three different areas of the ECAL Barrel. The curves, from bottom to top, represent the accuracy for low, middle and high $\eta$ regions in the ECAL Barrel. As can be seen, an inter-calibration precision of 0.6% averaged over the Barrel can be achieved with 10 $fb^{-1}$ of integrated luminosity.

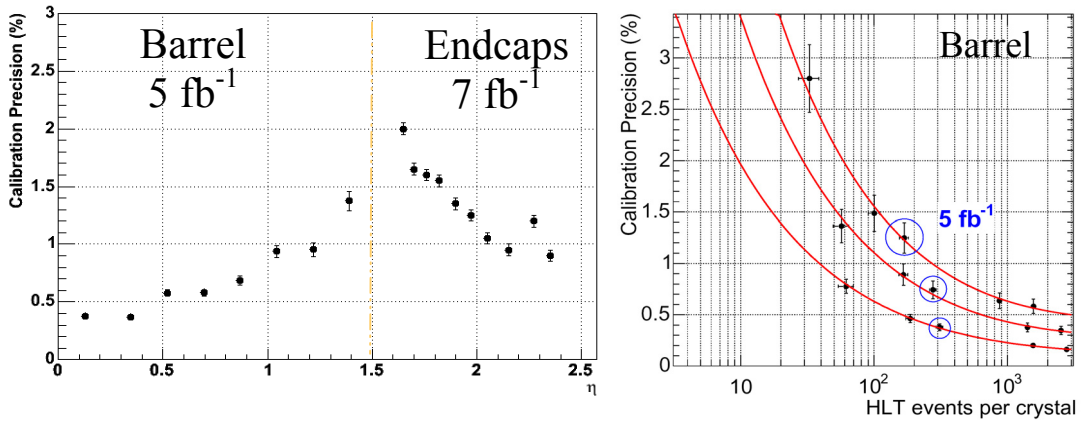


(a) (b)

**FIGURE 4.** (a) Calibration precision versus η using isolated electrons (b) Calibration precision versus HLT events per crystal for different η Barrel regions. Upper curve: the last 10 crystals in the Barrel ($1.305<\eta<1.479$); middle curve: 10 crystals in the middle of the Barrel ($0.783<\eta<0.957$); lower curve: the first 15 crystals in the Barrel ($0.0<\eta<0.261$). The third point along each line gives the precision of 5 $fb^{-1}$ of integrated luminosity.

After crystals within regions of η are inter-calibrated, the regions have to be calibrated among themselves. This task is accomplished by selecting electrons with minimum energy loss due to bremsstrahlung. After this selection, the resulting values of the peaks of the S25/P distributions that are found are consistent with the pseudorapidity dependence of shower containment.

The rate of the jet background in the single electron trigger stream (HLT output) is estimated to be 27Hz at low luminosity out of which 16Hz are expected in the Barrel. The residual background has been investigated for the Barrel case. After the calibration selection is applied, the surviving background corresponds to a rate of 2.3 Hz. One third of this rate comes from b/c→e semileptonic decays. Such decays might be useful in the calibration process, increasing the overall calibration statistics. If required, the background can easily be further reduced by a factor 10, using isolation cuts, with only a small effect on the signal efficiency.

## Calibration with $\pi^0,\eta\rightarrow\gamma\gamma$ and $Z\rightarrow\mu\mu\gamma$

The possibility of inter-calibrating the ECAL using the reconstructed mass of $\pi^0,\eta\rightarrow\gamma\gamma$ is being investigated. These low mass particles could provide an important additional calibration tool which is useful for relatively rapid inter-calibration of all crystals, study of the effects of crystal transparency corrections from the laser monitor and rapid check-out and monitoring of detector performance.

The inter-calibration obtained from low-energy $\pi^0\rightarrow\gamma\gamma$ is not sensitive to Tracker material if unconverted photons are selected. The only effect of the Tracker material is a rate loss at larger η values due to photon conversions.

It has been shown that $\pi^0$s, useful for calibration, can be located within events using the ECAL Level-1 trigger information, requiring very little processing time to extract

the small amount of information relevant for calibration. In the ECAL Barrel, the $\pi^0$ mass peak, with relatively little background, has a mass resolution of about 8%. Around 1.4% of the Level-1 trigger events have a usable $\pi^0$ in the Barrel and almost all of them are tagged by the isolated electron Level-1 trigger. With an assumed Level-1 global trigger rate of 25 kHz, about 100 $\pi^0$s per crystal can be obtained in a running period of less than 5 hours.

Events from $\eta\rightarrow\gamma\gamma$ are also being studied. The signal has a much lower rate once the background is reduced sufficiently, but the mass resolution is about 3%. The $\eta\rightarrow\gamma\gamma$ decay should be a useful calibration tool at higher energy and may prove very useful in the Endcaps, although it will take longer.

A significant rate of high-$P_T$ photons with very little background and an energy that can be known independently of the ECAL, is available in radiative decays of $Z\rightarrow\mu\mu$. These photons are being investigated as a valuable tool for various calibration related tasks, as well as a probe for measuring photon reconstruction efficiency. They can be used, for example, to inter-calibrate different regions of the ECAL (coefficient $c_i$ of Equation 2), and to tune the various cluster correction algorithms (coefficient $F$) and the overall energy scale (coefficient $G$). They can also be used to relate the energy scale of unconverted photons to that of electrons (from converted photons). For an integrated luminosity of only 1 $fb^{-1}$, an average of nearly 1 such photon per crystal will be collected.

## Summary

The calibration of the CMS crystal calorimeter will be performed before and after the assembly of the detector. Before the assembly, crystals will be calibrated in the Testbeam, using laboratory measurements and with cosmic muons. After the assembly, crystals will be calibrated using physics events. At startup, the φ-uniformity inter-calibration technique will provide a precision of around 2% in a couple of hours. The design precision of 0.5% will be achieved using the E/P ratio of isolated electrons mainly from W and Z decays. The mass reconstruction of $\pi^0$,$\eta\rightarrow\gamma\gamma$ and $Z\rightarrow\mu\mu\gamma$ will provide important additional calibration tools.

## REFERENCES


1. CMS Collaboration,"The Electromagnetic Calorimeter Technical Design Report", *CERN/LHCC* **97-033**.
2. CMS Collaboration,"The Magnet Project Technical Design Report", *CERN/LHCC* **97-010**.
3. CMS Collaboration,"The Tracker Project Technical Design Report", *CERN/LHCC* **98-006**.
4. CMS Collaboration,"The Muon Project Technical Design Report", *CERN/LHCC* **97-032**.
5. CMS Collaboration,"The CMS Physics Technical Design Report, Volume I", *CERN/LHCC* **2006-001.**
6. CMS Collaboration,"The CMS Physics Technical Design Report, Volume II", *CERN/LHCC* **2006-021.**
7. P. Adzic et al., "Results of the first performance tests of the CMS e/m calorimeter", *Eur. Phys. J.* **C44**, s02, 1-10 (2006).
8. M. Bonesini et al. "Inter-calibration of the CMS e/m calorimeter with cosmic rays before installation", *CMS Note* **2005/023**.
9. D. Futyan et al. "Intercalibration of ECAL crystals in φ Using Symmetry of Energy Deposition", *J. Phys.* **G29** (2003) 1229-1236.
10. D. Futyan, "Intercalibration of the CMS e/m calorimeter using jet trigger events", *CMS Note* **2002/031**.
11. R. Paramatti et al. "Use of $Z\rightarrow e^+e^-$ events for ECAL calibration", *CMS Note* **2006/039**.
12. L. Agostino et al. " Intercalibration of the CMS e/m calorimeter with isolated electrons", *CMS Note* **2006/021**.